Ab initio study of W-Al-Co-Ni: An approximant of the decagonal Al-Co-Ni quasicrystal

Kai H. Hassdenteufel,[1] Artem R. Oganov,[1,3] Sergiy Katrych,[2] and Walter Steurer[1,*]
[1]*Laboratory of Crystallography, Department of Materials, ETH Zurich, Wolfgang-Pauli-Strasse 10, CH-8093 Zurich, Switzerland*
[2]*Laboratory of Solid State Physics, Department of Physics, ETH Zurich, Schaffmattstrasse 16, CH-8093 Zurich, Switzerland*
[3]*Geology Department, Moscow State University, 119992 Moscow, Russia*
(Received 26 September 2006; revised manuscript received 19 February 2007; published 30 April 2007)

We have performed *ab initio* simulations of binary and ternary periodic model structures based on the W phase in order to investigate chemical bonding, its response to pressure, and structural relaxations accompanying the substitution of Co by Ni. Our results support previous conclusions that the maximization of Al-Co and Ni-Ni interactions is favorable for reaching the lowest-energy state. The valence electron localization function (ELF) indicates partially covalent bonding supporting the formation of energetically favorable atomic clusters. The existence of a pseudogap in the calculated electronic density of states close to the Fermi level suggests electronic stabilization according to the Hume-Rothery-type mechanism. High-pressure simulations of binary W-(Al,Co) up to 90 GPa reveal increasing puckering of the atomic layers perpendicular to the pseudotenfold *b* axis. Furthermore, the basic pentagonal columnar clusters become distorted, leading to shorter distances between neighboring Co atoms. The structural changes in the vicinity of the distorted clusters point to local changes in the chemical bonding as reflected in the valence ELF.

DOI: 10.1103/PhysRevB.75.144115 PACS number(s): 61.43.Bn, 61.44.Br, 62.50.+p, 71.15.Mb

I. INTRODUCTION

The decagonal phase in the system Al-Co-Ni shows a very broad stability range of approximately 20 at. % concerning the Co/Ni concentration. Furthermore, there exist several complex periodic as well as quasiperiodic ordering states as a function of the Co/Ni ratio.[1] The origin of the stability of the decagonal phase is still discussed controversially. In particular, the role of basic clusters observed by electron microscopy is not clear. For a recent discussion of this topic see Ref. 2.

Up to date the fundamental question has remained open, whether quasiperiodic long-range order can be a ground state of matter or is possible only in entropy-stabilized high-temperature (HT) phases. To answer the question of the low-temperature (LT) stability of decagonal Al-Co-Ni, several studies were performed such as *in situ* LT single-crystal x-ray diffraction (XRD) and high-pressure (HP) long-term LT annealing experiments.[3] No transition to a periodic phase has been detected so far, probably due to the sluggish kinetics (for a review see Ref. 4). In order to enhance atomic mobility by ballistic diffusion, ball milling experiments were performed.[5] This method was successfully applied to other quasicrystals inducing phase transformations.[5–8] However, the resulting samples are highly defective and contain impurities from the milling equipment. Therefore, the observed phase changes cannot be taken as evidence against zero-kelvin stability of quasicrystals. For topological reasons, the transformation from a quasiperiodic to a periodic state always involves diffusion of atoms. Consequently, it is impossible to reach by this kind of experiments a LT equilibrium state. More reliable information on the stability of quasicrystals and the underlying stabilization mechanism can be obtained from quantum mechanical calculations. For example, the ground-state structure can be established by a combination of experiment and *ab initio* calculations[9,10] or even purely theoretically using the recently developed *ab initio* evolutionary methodology.[11–13] We studied by *ab initio* simulations the stability of binary and ternary model structures based on the W phase at ambient pressure as well as under high pressures, up to 90 GPa.

II. METHODOLOGY

We have performed *ab initio* simulations using VASP (Vienna *ab initio* simulation package),[14,15] within the generalized gradient approximation (GGA).[16] The following all-electron projector-augmented wave (PAW) potentials have been used for the atoms, all derived within the same GGA functional: core region cutoffs are 1.9 a.u. for Al (core configuration $1s^1 2s^2 2p^6$) and 2.3 a.u. for Co and Ni (core configuration $1s^2 2s^2 2p^6 3s^2 3p^6$). A plane-wave kinetic energy cutoff of 270 eV was used for optimization, and a larger cutoff of 350 eV was used for accurate calculation of the valence electron localization function (ELF) and the electronic density of states (DOS) of the optimized structure. The conjugate-gradients and steepest-descent methods were used for relaxation of the structures. The self-consistency threshold for electronic optimization was 5×10^{-4} eV per unit cell (532 atoms); structural relaxation proceeded until forces acting on atoms were well below 0.05 eV/Å. All total-energy calculations were the done with the Γ point for Brillouin-zone sampling. Methfessel-Paxton electronic smearing[17] was used with a smearing width of 0.2 eV to facilitate convergence. For accurate calculations of the electronic density of states, we used the charge density obtained in the Γ-point calculation and performed a non-self-consistent (i.e., keeping the charge density fixed) calculation with a $2 \times 4 \times 2$ *k* mesh used for Brillouin-zone sampling.

HP simulations were performed to investigate the influence of pressure on the structure. However, when using finite basis sets, VASP (as well as any plane-wave-based code) underestimates pressure. This effect is called the Pulay stress. Since the errors are almost isotropic, the simulations can be

 ©2007 The American Physical Society

easily corrected for the Pulay stress. For the plane-wave cutoff used in this work (270 eV), the Pulay stress was calculated to be 0.8 GPa. Afterwards, HP simulations were conducted, increasing the pressure from 0 GPa to 100 GPa. The positions of the atoms and the lattice parameters were equilibrated while keeping the space group symmetry. At 100 GPa, the forces on atoms could not be reduced below 0.05 eV/Å and the simulation was stopped after more than 200 relaxation steps. Visualization of the ELF was performed with the STM3 package.[18]

III. STRUCTURAL MODELS

Since periodic boundary conditions have to be applied, the quasiperiodic structure itself (if it was known) cannot be modeled directly, because the unit cell is infinite in three-dimensional physical space. For this reason, periodic model structures were used based on the structure of the W phase,[19] which is the largest stable approximant in the system Al-Co-Ni with nominal composition $Al_{71.8}Co_{21.1}Ni_{7.1}$. The monoclinic crystal structure [space group *Cm*, $a=39.668(3)$ Å, $b=8.158(1)$ Å, $c=23.392(1)$ Å, $\beta=90.05(1)$] was first described by Sugiyama *et al.*[20] It consists of two types of atomic layers, stacked along the pseudotenfold *b* axis: flat layers at $y=0$ and 1/2 and puckered layers at $y \approx 1/4$ and 3/4. The layer at $y=1/2$ is related to the one at $y=0$ by a shift of 1/2 along the *a* axis (a result of *C* centering). The puckered layers are related to each other by a mirror plane.

The structure of the W phase is closely related to that of the decagonal quasicrystal, even though it is not a rational approximant. Both structures contain the same features: 20-Å clusters (i.e., structural building units) with 8-Å periodicity, consisting of subclusters formed by pentagonal prisms and antiprisms. Unfortunately, nothing is known about the Co/Ni ordering, since these elements cannot be distinguished by XRD due to their similar atomic scattering factors. For this reason, binary (Al, Co) and (Al, Ni) models of the W phase were used as a starting point.[34] Our model structures were set up from in-house single-crystal XRD data. Hereafter, these models are referred to as W-(Al,Co) and W-(Al,Ni). To investigate the effect of pressure on the structure and its building units, we also performed high-pressure simulations of the binary W-(Al,Co) structure.

The results of the simulations of the binary models were used to set up a realistic ternary model of the W phase. According to first-principles-based calculations of Al-Al, Al-Co, Al-Ni, Co-Co, Ni-Ni, and Co-Ni pair potentials, Al-Co and Ni-Ni interactions are energetically preferred compared to the other ones.[21] To test this finding, two different models were investigated, which differ only by their Co/Ni distribution. While in the first model (referred to as model 1) the transition metal (TM) sites with largest distances were occupied by Co to maximize the number of Al-Co and Ni-Ni bonds, a second model (model 2) was created in which the TM atoms were distributed to maximize the number of Al-Ni and Co-Co bonds. For both models, the chemical composition and local fivefold symmetry were preserved. Simulations showed that the second model is less preferable, supporting the results of Ref. 21.

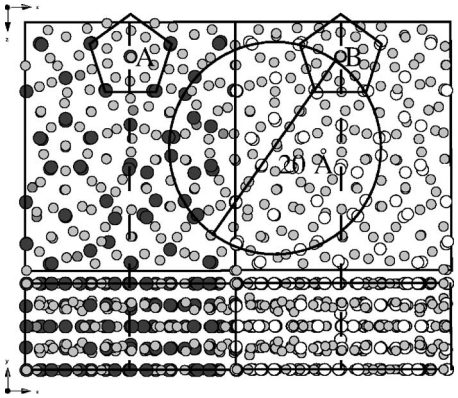

FIG. 1. Relaxed structures of W-(Al,Co) (left) and W-(Al,Ni) (right) (Al, light gray circles; Co, dark gray circles; Ni, open circles), projected along [010] (top) and [001] (bottom); half of the unit cell along the *a* axis is shown for each structure; the 20-Å cluster is encircled; the pentagonal subclusters marked *A* and *B* show the most significant differences.

Recently, Mihalkovič and Widom[22] published a structure model of the W phase. They used *ab initio* calculations to refine the chemical ordering of the W phase (for structural information and the results of the total-energy calculations, see Ref. 35). The model with the lowest total energy shows a chemical composition of $Al_{380}Co_{110}Ni_{40}$, two Co atoms fewer than the models of the present study. It looks similar to our model 1 with differences mainly in the Co/Ni distribution. Contrary to our models, the model published in Ref. 22 contains a mixed Al/Ni site, which breaks the space group symmetry *Cm*.

IV. ATOMIC STRUCTURE

A. Binary W-(Al,Co) and W-(Al,Ni)

At first glance, the structures of the two binary models look very similar (Fig. 1). There are only small atomic shifts visible, well below 0.1 Å for both Al and TM atoms. The largest shifts occur for the atoms involved in the formation of one specific pentagonal subcluster, marked by the letters *A* and *B* in Figs. 1 and 2. Five atoms in the second coordination

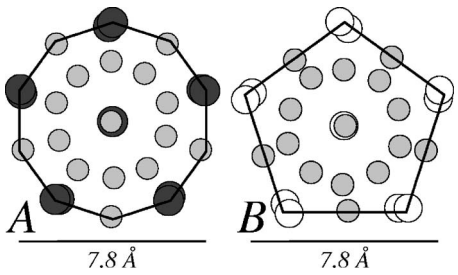

FIG. 2. Enlarged section of Fig. 1 showing the variation of the pentagonal subcluster with Co/Ni substitution: W-(Al,Co) (left) and W-(Al,Ni) (right) (Al, light gray circles; Co, dark gray circles; Ni, open circles).

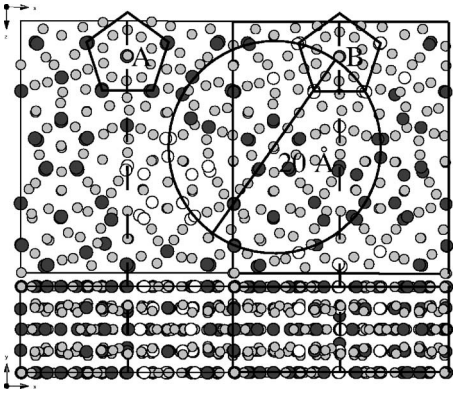

FIG. 3. Optimized structure of ternary W-$Al_{380}Co_{112}Ni_{40}$, model 1 (left) and model 2 (right), view along [010] (top) and [001] (bottom); half of the unit cell along the *a* axis is shown for each structure (Al, gray circles; Co, solid circles; Ni, open circles).

sphere move from the corners of a regular decagon in case of W-(Al,Co) (left, marked *A*) to the edge centers of a pentagon in the structure of W-(Al,Ni) (right, marked *B*). While the Al atoms move towards the center by almost 1 Å, the TM atoms move slightly away from the center. The central TM atom moves 0.447 Å out of plane of the puckered layer, increasing the puckering. The atomic displacements found in our simulations corroborate the interaction model of Co and Ni: Co shows a stronger attractive force than Ni in Al-TM interactions and a more repulsive one in TM-TM interactions.

B. Ternary W-$Al_{380}Co_{112}Ni_{40}$

The optimized structures of the ternary models 1 and 2 are very similar (Fig. 3). Only the TM atom in the center of the pentagonal subclusters *A* and *B* shows a significant difference. In case of Co, it is shifted out of plane by 0.347 Å in model 1, increasing to 0.735 Å in model 2. The reason for that is in the change of TM coordination. Also the lattice parameters of the ternary models (Table I) change with the Co/Ni distribution, *b* by 0.4%, *a* and *c* by 0.7%.

Since both models have the same chemical composition, their total energies can be directly compared. Accordingly, the total energy of model 1, for which the TM sites with shortest TM-TM distances are occupied by Ni, is by about 0.049 eV per atom below model 2, in which the sites with largest TM-TM distances are occupied by Ni. Thus, the total energy of the system can be reduced if Co is surrounded by Al only and neighboring TM sites are occupied by Ni. These results are consistent with earlier suggestions.[21,23]

TABLE I. Lattice parameters of ternary models of W-$Al_{380}Co_{112}Ni_{40}$ (after structural optimization).

	a[Å]	*b* [Å]	*c* [Å]	β [deg]
Model 1	39.568	8.024	23.368	89.884
Model 2	39.828	8.059	23.528	89.874
Experiment	39.668	8.158	23.392	90.1

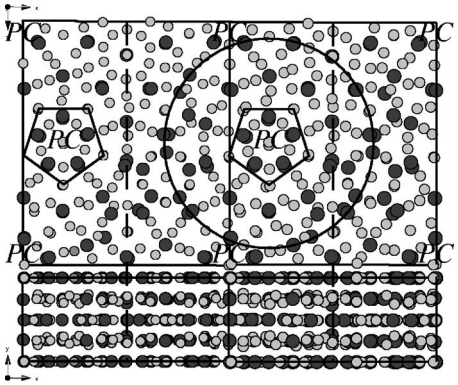

FIG. 4. Structure of W-(Al,Co), relaxed at zero GPa (left) and 90 GPa (right) (Al, light gray circles; Co, dark gray circles), view along [010] (top) and [001] (bottom); half of the unit cell along the *a* axis is shown for each structure; PC marks the center of distorted pentagonal subclusters.

C. Influence of pressure on binary W-(Al,Co)

HP simulations show only marginal changes of the structure with increasing pressure, corroborating the experimental results.[24] A slight distortion of the pentagonal subclusters (marked PC in Fig. 4) takes place under pressure. Al-Al, Al-Co, and Co-Co distances decrease uniformly with pressure while the puckering of the layers increases. The lattice parameters *a* and *c* change by about 12% and the *b* axis by 10% only (Table II), leading to an enhanced puckering at higher pressure. The angle β remains nearly constant up to 90 GPa.

V. ELECTRONIC STRUCTURE

A. Electronic density of states

The plots of the calculated electronic DOS of the binary and ternary models are shown in Fig. 5. Two distinct peaks are present in the DOS for both ternary models corresponding to the *d* bands of Co and Ni (Fig. 5). Their energies are 2.50 eV and 1.85 eV below the Fermi level for model 1 and 2.65 eV and 1.79 eV for model 2, respectively. The DOS of the binary models shows a maximum at −1.80 eV for W-(Al,Co) and −2.98 eV for W-(Al,Ni), relative to the Fermi level. The plots show that strong Ni-Ni and Al-Co interactions shift the total DOS and the peaks to lower energies, in agreement with the results of Krajči *et al.*[23]

TABLE II. Lattice parameters of binary W-(Al,Co) with increasing pressure (after structural optimization).

p [GPa]	*a* [Å]	*b* [Å]	*c* [Å]	β [deg]
0	39.635	7.987	23.404	89.873
20	38.027	7.710	22.447	89.852
40	36.975	7.517	21.825	89.847
60	36.162	7.368	21.344	89.838
80	35.533	7.250	20.971	89.830
90	35.214	7.201	20.793	89.818

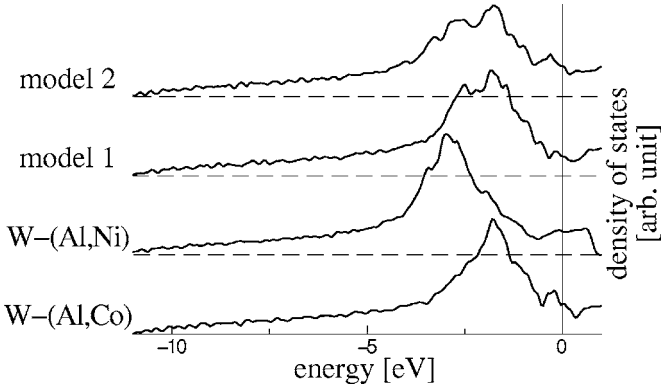

FIG. 5. DOS of binary W-(Al,Co) and W-(Al,Ni) in comparison with the DOS of models 1 and 2 of ternary W-$Al_{380}Co_{112}Ni_{40}$; strong Ni-Ni and Al-Co interactions shift the total DOS to lower energies; zero energy is set to the Fermi level.

Looking at the shape of the peaks of the DOS, a shoulder is present some 10 meV next to the peak for both binary and ternary models. Earlier, this was found to be due to splitting of the TM *d* band resulting from Al (*s*,*p*)–TM (*s*,*d*) hybridization, thereby lowering the energy of corresponding electrons.[23] Furthermore, all models possess two pseudogaps close to the Fermi level except for W-(Al,Ni) which shows just a smooth one at approximately 0.60 eV below the Fermi level. In the DOS of binary W-(Al,Co), one pseudogap exists at −0.50 eV relative to the Fermi level and another deeper one at 0.33 eV above the Fermi level. The DOS of model 1 shows a weak pseudogap at −0.37 eV and another one at 0.28 eV. The positions of the pseudogaps of model 2 are −0.73 eV and 0.19 eV, separated by a peak. The existence of a pseudogap close to the Fermi level in the electronic DOS points to a Hume-Rothery-type stabilization of the structure.

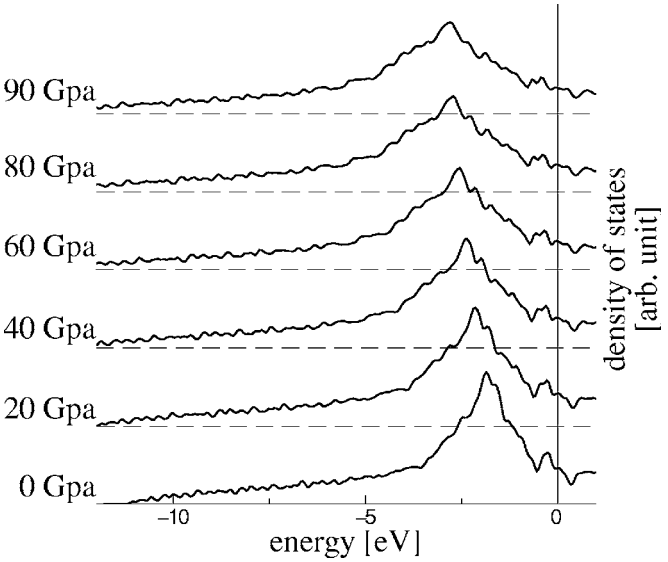

FIG. 6. DOS of W-(Al,Co) as a function of pressure; separation of a shoulder at higher energies with increasing pressure (marked by the dashed line) caused by the distortion of the pentagonal subclusters (marked PC in Fig. 4); zero energy is set to the Fermi level.

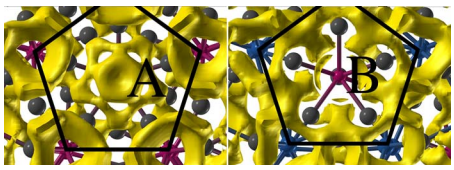

FIG. 7. (Color online) (Al, gray; Co, red; Ni, blue) Valence ELF (isosurface at a level of 0.6) of ternary W-$Al_{380}Co_{112}Ni_{40}$, model 1 (left) and model 2 (right); the subclusters marked *A* and *B* in Fig. 3 are shown.

Krajči *et al.*[23] calculated the electronic DOS of two different structures, both based on the W phase as well. They report a deep minimum (pseudogap) at the Fermi level for the model with composition of $Al_{189}Co_{39}Ni_{39}$, while the pseudogap is 0.09 eV above the Fermi level for the model with the experimentally determined composition of the W phase. They concluded that the pseudogap is rather insensitive to the Co/Ni composition. While we did not investigate different compositions, our results show that the position and shape of the pseudogap change with the Co/Ni distribution.

Figure 6 shows the electronic DOS of W-(Al,Co) as a function of pressure. Major changes are only visible in the vicinity of the maximum of the curves. With increasing pressure, the peak broadens and a side peak at the right of the maximum moves to higher energies. This is mainly due to local changes of the structure—i.e., the distortion of the pentagonal subclusters marked by PC in Fig. 4. The distortion weakens the Al-Co interaction and forces closer Co-Co contacts. These move electrons to higher energies, leading to an additional peak separating increasingly from the maximum with pressure. The pseudogaps persist under pressure. However, a flattening of the DOS at the Fermi level takes place with increasing pressure, also lowering the depth of the pseudogaps. Thus, pressure weakens the Hume-Rothery-type stabilization.

B. Electron localization function

The ELF[25,26] is strongly related to the Pauli principle and visualizes the localization of electrons of the same spin. Thus, it allows for studying the nature of chemical bonding in a material. The valence ELF of optimized structures shows distinct deviations from that of free-electron metals, which have an ELF value of 0.5 everywhere. In our case (Fig. 7), valence electrons are localized between TM and Al atoms, as

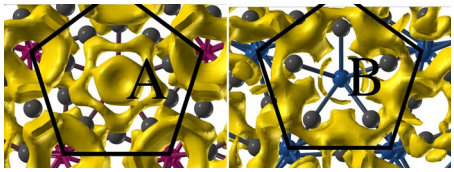

FIG. 8. (Color online) (Al, gray; Co, red; Ni, blue) Valence ELF (isosurface at a level of 0.6) of W-(Al,Co) (left) and W-(Al,Ni) (right); the subclusters marked *A* and *B* in Figs. 1 and 2 are shown. Remarkably, the ELF in model 2 is similar to that in W-(Al,Ni), although Co is present in the center of this cluster in both ternary models.

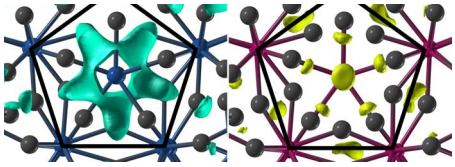

FIG. 9. (Color online) The images show different ELF sections of the subcluster *A* of Fig. 8. The ELF of W-(Al,Ni), calculated by substituting Co by Ni without further relaxation, was subtracted from the ELF of W-(Al,Co). In the left image the isosurfaces are shown at the level of −0.2, in the right image at +0.2.

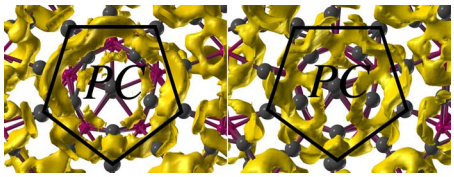

FIG. 10. (Color online) (Al, gray; Co, red; Ni, blue) Valence ELF (isosurface at a level of 0.6) of the cluster marked PC in Fig. 4 for W-(Al,Co) at 0 GPa (left) and 90 GPa (right), view along [010].

well as between neighboring Al atoms, indicating contributions from covalent bonding. No localization appears between neighboring TM atoms. Krajči *et al.*[23,27–31] also report the existence of localized electrons between Al and TM atoms and weaker electron localization between neighboring Al atoms. The formation of covalent bonding is due to the Hume-Rothery mechanism, leading to the formation of energetically favorable local arrangements of atoms (clusters). No differences are visible for those areas of the structure, in which the Co/Ni distribution has not changed. However, distinct changes of the valence ELF appear in the pentagonal subclusters depicted in Fig. 2.

Comparing the valence ELF of the ternary and binary models (Figs. 7 and 8), the ELF of model 1 looks similar to that of W-(Al,Co), while the valence ELF in model 2 is similar to that in W-(Al,Ni), although Co is present in the center of this cluster in both ternary models. Thus, the difference in the electron localization must be due to the change of the distribution of Co and Ni, which show very different interactions with neighboring atoms. For investigating the influence of a different TM site occupation, the valence ELF was also calculated for the relaxed structure of W-(Al,Co), in which Co was replaced by Ni without further relaxation. The resulting ELF of this model was subtracted from that of the original model containing Co only and the difference plotted (Fig. 9). This illustrates the change of electron localization in that area. Negative values of the difference ELF indicate the regions with higher electron localization for the Ni-substituted structure, while positive values mark those areas in the relaxed W-(Al,Co) structure.

The valence ELF changes significantly with pressure. In Fig. 10, the valence ELF of the cluster marked PC in Fig. 4 for W-(Al,Co) at zero GPa (left) and 90 GPa (right) is given. Neither at 0 GPa nor at 90 GPa, electrons are localized between neighboring Co atoms. Generally, the electron localization between Al atoms does not change at all with increasing pressure while that between Co and Al atoms decreases. This indicates a weaker covalent bonding between them, pointing to a decrease of the Al (s,p)–Co (s,d) hybridization. The change of the valence ELF with increasing pressure thus supports the conclusion drawn from the change of the DOS: closer Co-Co distances move the electrons to higher energies because of the repulsive Co-Co interactions.

VI. CONCLUSIONS

The stabilization of the basic building units, the pentagonal subclusters, was found to be due to hybridization between neighboring Al atoms as well as covalent bond formation between Al and TM atoms. This was found for other quasicrystal models as well.[23,27–31] The calculated DOS reveals the existence of a pseudogap, pointing to a possible contribution of the Hume-Rothery mechanism to the stabilization of the structure. However, a Hume-Rothery-type stabilization is not the only contribution to the stabilization of the structure. Maximization of energetically favorable Ni-Ni and Al-Co interactions certainly plays a role as well.

Sheng *et al.*[32] investigated the short-range order in binary metallic glasses. They found that the forming clusters are stabilized by covalent bonding between atoms of different species, thereby lowering the energy of the cluster. Thus, maximizing the number of unlike bonds will reduce the total energy of the system. This is best achieved if solute atoms are surrounded by solvent atoms only, which is possible up to a certain concentration of the solute atoms. At higher concentrations, the solute atoms form pairs, rings, and strings, leading to medium-range order.

This is similar for the distribution of Co and Ni atoms in the W phase: The TM atoms are surrounded mostly by Al atoms to maximize the number of Al transition metal bonds. Because of the high concentration of nearly 30 at. %, there are only a few TM sites, where the TM atom can be surrounded by Al only. Most TM atoms are connected in pairs and five rings, as well as strings running along the stacking direction of the layers.

The HP simulations of binary W-(Al,Co) reveal that the structural building units get slightly distorted with pressure, leading to an energetically unfavorable increasing Co-Co interaction. That causes additional peaks in the DOS and the formation of a shoulder at higher energies. The change of the covalent bonding is also visible in the valence ELF. Furthermore, enhanced puckering was found with increasing pressure due to different responses of the lattice parameters, consistent with resonant ultrasound spectroscopy measurements of decagonal Al-Co-Ni.[33]

ACKNOWLEDGMENTS

K.H.H. expresses his gratitude to D. Adams and D. Y. Jung for valuable discussions and Mario Valle for visualization. We thank CSCS (Manno) for computational facilities and the Swiss National Science Foundation for funding (Grant No. 200020-105158) and computational facilities.

*Correspondence: steurer@mat.ethz.ch

[1] W. Steurer, Z. Kristallogr. **219**, 391 (2004).
[2] W. Steurer, Philos. Mag. **86**, 1105 (2006).
[3] K. H. Hassdenteufel and W. Steurer, Philos. Mag. **86**, 355 (2006).
[4] W. Steurer, Acta Crystallogr., Sect. A: Found. Crystallogr. **61**, 28 (2005).
[5] N. K. Mukhopadhyay, T. P. Yadav, and O. N. Srivastava, Philos. Mag. Lett. **83**, 423 (2003).
[6] N. K. Mukhopadhyay, T. P. Yadav, and O. N. Srivastava, Philos. Mag. A **82**, 423 (2002).
[7] N. K. Mukhopadhyay, G. V. S. Murthy, B. S. Murty, and G. C. Weatherly, J. Alloys Compd. **342**, 38 (2002).
[8] N. K. Mukhopadhyay, G. V. S. Murthy, B. S. Murty, and G. C. Weatherly, Philos. Mag. Lett. **82**, 283 (2002).
[9] A. R. Oganov and S. Ono, Nature (London) **430**, 445 (2004).
[10] A. R. Oganov and S. Ono, Proc. Natl. Acad. Sci. U.S.A. **102**, 10828 (2005).
[11] A. R. Oganov, C. W. Glass, and S. Ono, Earth Planet. Sci. Lett. **241**, 95 (2006).
[12] A. R. Oganov and C. W. Glass, J. Chem. Phys. **124**, 244704 (2006).
[13] C. W. Glass, A. R. Oganov, and N. Hansen, Comput. Phys. Commun. **175**, 713 (2006).
[14] G. Kresse and J. Furthmuller, Comput. Mater. Sci. **6**, 15 (1996).
[15] G. Kresse and J. Furthmuller, Phys. Rev. B **54**, 11169 (1996).
[16] J. P. Perdew, K. Burke, and M. Ernzerhof, Phys. Rev. Lett. **77**, 3865 (1996).
[17] M. Methfessel and A. T. Paxton, Phys. Rev. B **40**, 3616 (1989).
[18] M. Valle, Z. Kristallogr. **220**, 585 (2005).
[19] K. Hiraga, T. Ohsuna, W. Sun, and K. Sugiyama, J. Alloys Compd. **342**, 110 (2002).
[20] K. Sugiyama, S. Nishimura, and K. Hiraga, J. Alloys Compd. **342**, 65 (2002).
[21] I. Al-Lehyani, M. Widom, Y. Wang, N. Moghadam, G. M. Stocks, and J. A. Moriarty, Phys. Rev. B **64**, 075109 (2001).
[22] M. M. Mihalkovič and M. Widom, Philos. Mag. **86**, 557 (2006).
[23] M. Krajči, J. Hafner, and M. M. Mihalkovič, Phys. Rev. B **62**, 243 (2000).
[24] G. Krauss, R. Miletich, and W. Steurer, Philos. Mag. Lett. **83**, 525 (2003).
[25] A. Becke and K. Edgecombe, J. Chem. Phys. **92**, 5397 (1990).
[26] C. Gatti, Z. Kristallogr. **220**, 399 (2005).
[27] M. Krajči, J. Hafner, and M. M. Mihalkovič, Phys. Rev. B **56**, 3072 (1997).
[28] M. Krajči and J. Hafner, Phys. Rev. B **68**, 165202 (2003).
[29] M. Krajči and J. Hafner, Phys. Rev. B **67**, 052201 (2003).
[30] M. Krajči and J. Hafner, J. Non-Cryst. Solids **334&335**, 342 (2004).
[31] M. Krajči, J. Hafner, and M. M. Mihalkovič, Phys. Rev. B **73**, 134203 (2006).
[32] H. W. Sheng, W. K. Luo, F. M. Alamgir, J. M. Bai, and E. Ma, Nature (London) **439**, 419 (2006).
[33] M. A. Chernikov, H. R. Ott, A. Bianchi, A. Migliori, and T. W. Darling, Phys. Rev. Lett. **80**, 321 (1998).
[34] crystallographic data are available at http://www.crystal.mat.ethz.ch/research/publications
[35] http://alloy.phys.cmu.edu